9-19-2019

Synthesizing galactose modified polymeric nanoparticles for biofilm inhibition of Pseudomonas aeruginosa

Tyler R. Flockton
Rowan University

SYNTHESIZING GALACTOSE MODIFIED POLYMERIC NANOPARTICLES FOR BIOFILM INHIBITION OF *PSEUDOMONAS AERUGINOSA*

by

Tyler Flockton

A Thesis

Submitted to the
Department of Chemistry and Biochemistry
College of Science and Mathematics
In partial fulfillment of the requirement
For the degree of
Master of Science in Pharmaceutical Sciences
at
Rowan University
June 5, 2019

Thesis Chair: Lark Perez, Ph.D.

Dedications

I would like to dedicate this to my family. My mother, father, sister and grandmother were by myside through my college journey. My parents gave me a place to live for free while I was taking classes and doing research. They did whatever it took for me to be able to complete my masters with the least amount of worries outside of school.

I would also like to dedicate this to my fiancé. She put up with my long days, nights and research. She helped keep me on the straight and narrow while I was completing my graduate degree.

Acknowledgments

I first and foremost would like to acknowledge Dr. Lark Perez for guiding me throughout my two years of my graduate degree. He is my mentor that helped me through all of the tough times of research. If it was not for him, I would not be where I am at this point of my career. I learned so much under his watch, from general lab techniques to real life lessons.

Second, I would like to acknowledge Dr. Jonnalagadda for all the advice that he gave me throughout my undergraduate and graduate career. Lastly, I would like to acknowledge all of the students and staff in the Chemistry and Biochemistry department. Everyone was so nice and helpful for all of a graduate student's needs.

Abstract

Tyler Flockton
SYNTHESIZING GALACTOSE MODIFIED POLYMERIC NANOPARTICLES FOR BIOFILM INHIBITION OF *PSEUDOMONAS AERUGINOSA*
2018-2019
Lark Perez Ph.D.
Master of Science in Pharmaceutical Sciences

Treating patients with antibiotics is becoming harder with the increase in antibiotic resistance. This is due to the widespread antibiotic use in clinical and agricultural settings. With antibiotic resistance outpacing new drugs making it to the market, developing new options to treat bacterial infections is and will be important. We created sugar modified nanoparticles to inhibit the biofilm formation of *Pseudomonas aeruginosa*.

P. aeruginosa is a gram-negative opportunistic pathogen that infects its host that has a compromised immune system. This makes it one of the most significant bacterial infection in hospitals. *P. aeruginosa* uses biofilms as an attack mechanism on the host. These biofilms are regulated through quorum sensing. Lec-A is the galactose binding lectin in *P. aeruginosa* which was the lectin target for this project. By knowing the binding pocket of the Lec-A, a galactose-modified di-block co-polymer is assembled into nanoparticles.

In order to make the nanoparticles to work better, more galactose modified sugars are added to the co-polymer. This was done by using Lysine to attach two galactose modified sugars to. The polymer was assembled by adding polymer to Cyanuric Chloride (TCT) then two lysines doubled modified galactose sugars to the TCT giving a tetra - modified polymer which will then be assembled to a nanoparticle.

Table of Contents

Table of Contents (Continued)

List of Figures

List of Tables

List of Schemes

Chapter 1

Inhibition of *Pseudomonas aeruginosa* Biofilm Formation with Surfaced Modified Polymeric Nanoparticles

1. Introduction

The ongoing increase of antibiotic resistance represents a significant challenge to modern medicine [1–3]. Due to the widespread use of antibiotics in clinical and agricultural settings and the limited number of novel antibiotics being advanced into the market, the development of new treatment options for bacterial infection is of paramount importance.

Pseudomonas aeruginosa represents one of the most significant gram-negative opportunistic pathogens involved in hospital-acquired infections. A report from the CDC-NNIS (National Nosocomial Infections Surveillance, US Dept. of Health and Human Services) identifies *P. aeruginosa* as the second leading cause of pneumonia, the third leading cause of urinary tract infection, and the eighth most frequently isolated pathogen from the bloodstream [1–7]. Further, *P. aeruginosa* often causes lethal infections in cystic fibrosis and immunocompromised patients, for whom the formation of bacterial biofilms plays a central role in infection and resistance [8,9]. Given the rapidly increasing incidence of *P. aeruginosa* in the clinic coupled with the high levels of antibiotic resistance and production of copious biofilms often found with this pathogen, the development of novel treatment strategies is imperative [10–12].

In *P. aeruginosa*, biofilm formation is regulated by a cell-cell communication mechanism known as quorum sensing, which is mediated by bacterial cell-surface lectins involved in cellular adhesion [13,14]. Specifically, the galactose-binding lectin LecA

(PA-IL) and the fucose-binding lectin LecB (PA-IIL) have prominent roles in bacterial virulence, cellular adhesion, tissue colonization, and/or invasion and biofilm formation [15–17]. Several recent reports have evaluated approaches to inhibit the virulence and/or biofilm formation in *P. aeruginosa* through inhibition of quorum sensing or lectin binding. Notable about these anti-virulence approaches is the potential they possess for species-selectivity by targeting the inhibition of cellular processes in a manner that uniquely inhibits the virulence and/or infectivity of *P. aeruginosa*. Accordingly, treatments developed for these *P. aeruginosa*-specific targets are anticipated to have a lower impact on the beneficial commensal bacterial population and may possibly exhibit reduced pressure for the development of antibiotic resistance.

Prior studies developing inhibitors of *P. aeruginosa* LecA have described mono-valent and multi-valent inhibitors of this lectin and have characterized the positive effect on inhibitor avidity through multivalency [12,17]. We rationalized that we might achieve similar high binding avidity for LecA using a polymeric nanoparticle with multiple copies of a LecA ligand on the surface of the particle. Further, we recognized that unlike dendrimeric or small molecule inhibitors of LecA, the surface-modified polymeric nanoparticles that we aimed to prepare would be capable of encapsulating a fluorescent or drug molecule within their lipophilic core, potentially enabling future applications in targeted antibiotic drug delivery or fluorescent labeling for diagnostic applications. Here we report our findings on the development and anti-biofilm properties of a series of LecA-targeted polymeric nanoparticles.

2. Results

2.1 Synthesis of galactose-modified di-block do-polymer. The D-galactose-modified di-block co-polymer required for nanoparticle assembly (**5**) was prepared from β-D-galactose pentaacetate in six steps (Scheme 1). In short, β-D-galactose pentaacetate (**1**) was coupled to benzyl 4-hydroxybenzoate (**2**) to provide ester **3**. Removal of the benzyl protecting group by hydrogenolysis provided carboxylic acid **4**, which was coupled to 6.6 kD amine terminated di-block co-polymer [18]. Removal of the acetate protecting groups on the sugar preceded purification of the sugar-modified polymer **1** by dialysis using a 5 kD molecular weight cutoff (MWCO) membrane. The resulting dialyzed D-galactose-modified polymer (**5**) was concentrated by lyophilization and the resulting white powder was characterized by NMR, IR, and MALDI-MS. Having prepared the requisite galactose-modified di-block copolymer **5**, we proceeded with the assembly of polymeric nanoparticles.

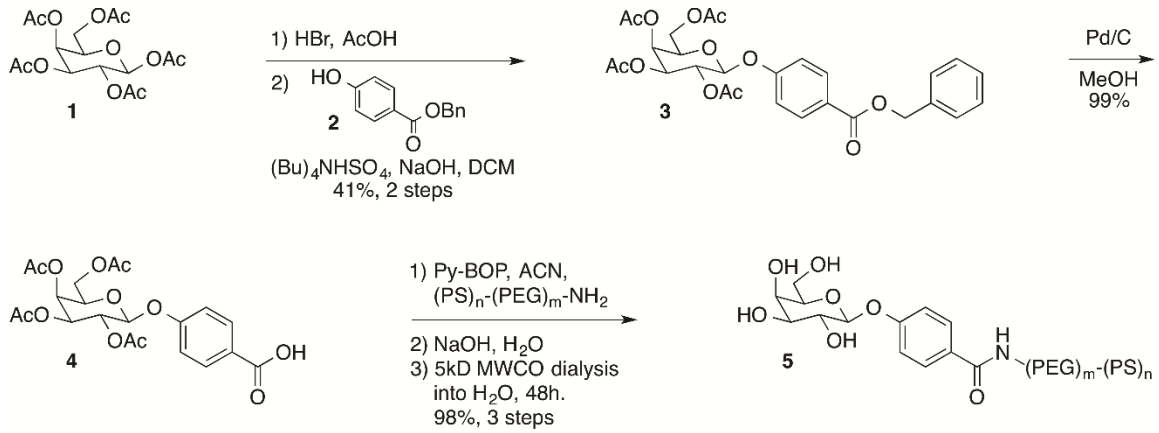

Scheme 1. Synthesis of modified di-block co-polymer for nanoparticle assembly. Abbreviations: DCM, dichloromethane; CAN, acetonitrile; MWCO, molecular weight cutoff

2.2 Nanoparticle preparation. Nanoparticles were prepared by flash nanoprecipitation using established methods [18,19] with varying ratios of the modified D-galactose polymer and unmodified di-block co-polymer to provide 100%-, 50%-, and 25%-surface-modified nanoparticles using the parameters described in Table 1. All nanoparticles were prepared using racemic α-tocopherol (vitamin E) as an inert core stabilizer.

Table 1.

Summary of polymeric nanoparticle (NP) prepared with varying levels of surface modification

Formulation	Active Stabilizer		Stabilizer		Inert Core		NP Properties	
	Block co-polymer	Conc. (mg/mL)	Block co-polymer	Conc. (mg/mL)	Filler	Conc. (mg/mL)	Z-diameter (nm)[1]	PDI[2]
0%	PS-*b*-PEG-Gal	0.00	PS-*b*-PEG	0.40	Vit E	0.40	88.83±4.64	0.0327
25% Gal-NP	PS-*b*-PEG-Gal	0.10	PS-*b*-PEG	0.30	Vit E	0.40	73.78±2.23	0.0132
50% Gal-NP	PS-*b*-PEG-Gal	0.20	PS-*b*-PEG	0.20	Vit E	0.40	74.74±2.26	0.0083
100% Gal-NP	PS-*b*-PEG-Gal	0.40	PS-*b*-PEG	0.00	Vit E	0.40	81.47±12.75	0.2693

Data represent the mean with error described as the standard error of means of at least three independent preparations of the particles, each with three instrumental replicates. [2] Polydispersity Index (PDI) = (standard deviation/mean diameter) ^2. Abbreviations: VitE, vitamin E (α-tocopherol).

All D-galactose nanoparticle (Gal-NP) suspensions were prepared as 0.02 mg/mL solutions in water and characterized in terms of particle diameters (Figure 1) and polydispersity indexes (PDI). The particles prepared are described in this manuscript based on the relative concentration of surface-modified D-galactose to enable direct comparison of the effect of the prepared nanoparticles on lectin binding and biofilm inhibition to free D-galactose, used as a control. Having prepared a series of galactose-modified polymeric nanoparticles, we conducted an evaluation of the lectin binding properties of the prepared particles.

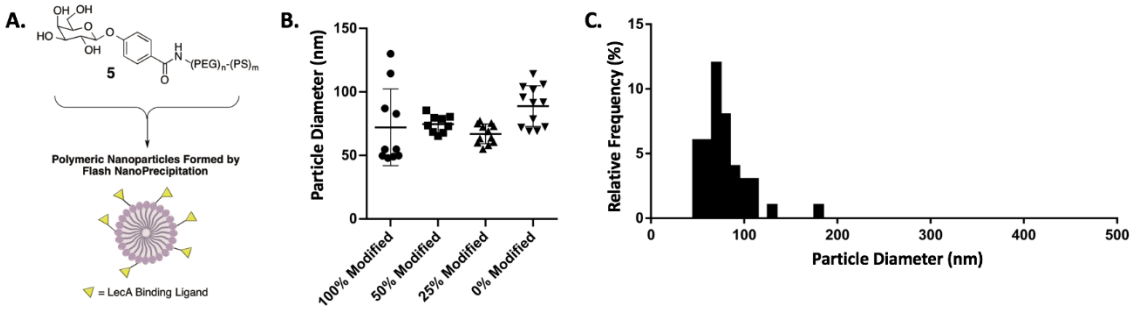

Figure 1. Schematic showing assembly of D-galactose surface-modified polymeric nanoparticles. B. Particle size distribution of prepared polymeric nanoparticles. Each data point represents the average particle diameter of an independent formulation. C. Histogram of particle size distribution for all nanoparticles prepared in this study.

2.3 Inhibition of LecA-mediated hemagglutination. The binding affinity of the modified nanoparticles for the *P. aeruginosa* lectin LecA was evaluated using a hemagglutination assay [20]. Briefly, this assay measures the inhibition of LecA-induced hemagglutination of rabbit erythrocytes by comparison with D-galactose as a control. The

exceptional effect of ligand multivalency was noted with the 100%- and 50%-modified NP samples, which were evaluated based on the concentration of galactose on the surface of the nanoparticles (Table 2). The strongest effect was observed with the 50%-modified Gal-NP, showing a 992-fold increase in relative potency compared with free galactose. The 100%-modified Gal-NP samples inhibited hemagglutination when modified with concentrations above 6.31μM of galactose, representing a 495-fold increase in potency relative to free galactose. The 25%-modified NP showed no inhibition of hemagglutination up to the highest surface concentration of D-galactose evaluated (2.36 μM). A control 100%-mannose-modified polymeric NP (37.9 μM mannose) showed no inhibition of hemagglutination, supporting the hypothesis that the inhibition of LecA is mediated by specific interactions between the lectin and the nanoparticle surface only with galactose modification.

Table 2.

Inhibition of P. aeruginosa LecA-induced hemagglutination.

Entry	Formulation	Hemagglutination Assay MIC (uM)[1]	Relative Potency[4]
1	D-galactose	3125.0	1.0
2	100%-Modified D-galactose-NP	6.31	495.2
3	50%-Modified D-galactose-NP	3.15	992.1
4	25%-Modified D-galactose-NP	none[2]	-
5	100%-Modified mannose-NP	none[3]	-

MIC = minimal inhibitory concentration for the hemagglutination assay following two-fold serial dilutions of tested compounds; the MIC corresponds to the highest dilution resulting in the inhibition of LecA-induced hemagglutination based on the relative sugar concentration. [2] No inhibition of hemagglutination up to highest concentration evaluated (galactose concentration of 2.36μM). [3] No inhibition of hemagglutination up to highest concentration evaluated (maltose concentration of 37.9μM). [4] Relative potency based on concentration of galactose = ($MIC_{(D\text{-}galactose)}/MIC_{(ligand)}$).

The high potency of the particles in this assay is consistent with previous reports of high avidity LecA binding using galactose modified dendrimers [12,20]. It is noted that the % modification of the particle leads to maximal inhibition with the 50%-sugar-modified particles. Particles with lower galactose modification (25%-modified) showed no inhibition of hemagglutination at the highest concentrations tested ([galactose] = 2.36 μM) and those with higher modification (100%-modified) had a two-fold higher MIC. It is possible that a sugar concentration greater than 2.36 μM on the nanoparticles is required for high avidity; however, higher sugar concentrations as would be present in the 100%-modified nanoparticles result in the steric inhibition of lectin binding.

2.4 Inhibition of P. aeruginosa PAO1 biofilm formation. Having identified that our 100%- and 50%-D-galactose-modified polymeric nanoparticles are effective at inhibiting LecA-induced hemagglutination, we evaluated their effect on bacterial biofilm formation using the well-established crystal violet assay [21,22]. Briefly, *P. aeruginosa* strain PAO1 was inoculated in 96-well plates in the presence of varying concentrations of Gal-NP, controls, and/or free D-galactose. Biofilm formation was evaluated after 24 h by removing non-adherent bacteria, crystal violet staining of the adherent cells, and determination of absorbance at 550nm. In this assay, we observed a potent dose-dependent inhibition of biofilm formation with our surface-modified Gal-NP samples (Figure 2). Inhibition of biofilm formation was noted at D-galactose concentrations above 12.6 μM in the 100%-surface-modified nanoparticle samples and at concentrations above 6.3 μM in the 50%-surface-modified series. Again, the significance of ligand valency is evident, as free D-galactose, even at 32,000 μM, showed no inhibition of biofilm formation in this assay.

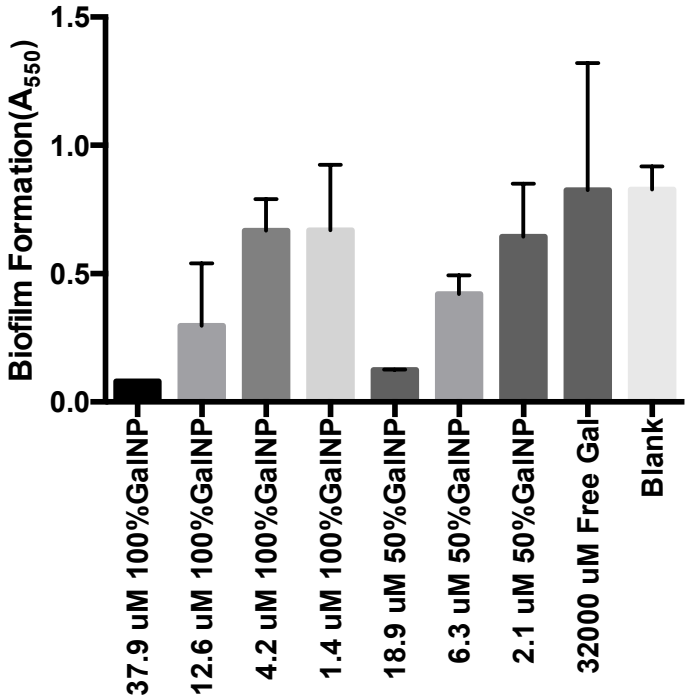

Figure 2. Inhibition of *P. aeruginosa* PAO1 biofilm formation based on the crystal violet assay. Surface-modified Gal-NP samples are described based on the % surface modification and the relative concentration of D-galactose on the nanoparticle surface. All data points are described as the mean of triplicate measurements with error bars representing the standard deviation.

2.5 Evaluation of growth inhibition. To confirm that the potent biofilm inhibitory activity observed was not due to growth inhibition by the nanoparticle samples evaluated, we collected full growth curve data for PAO1 by monitoring OD_{600} (Figure 3). We were surprised to find that the highest concentration of 100%- and 50%-modified nanoparticles (correlating to D-galactose concentrations of 75.8 μM and 37.8 μM, respectively) did potently inhibit bacterial growth. Despite this, no significant inhibition of growth was noted at any of the nanoparticle concentrations evaluated in our biofilm inhibition assay. The absence of growth inhibition supports the hypothesis that that nanoparticle-LecA

binding interactions inhibit bacterial biofilm formation via an antivirulence (non-antibiotic) mechanism.

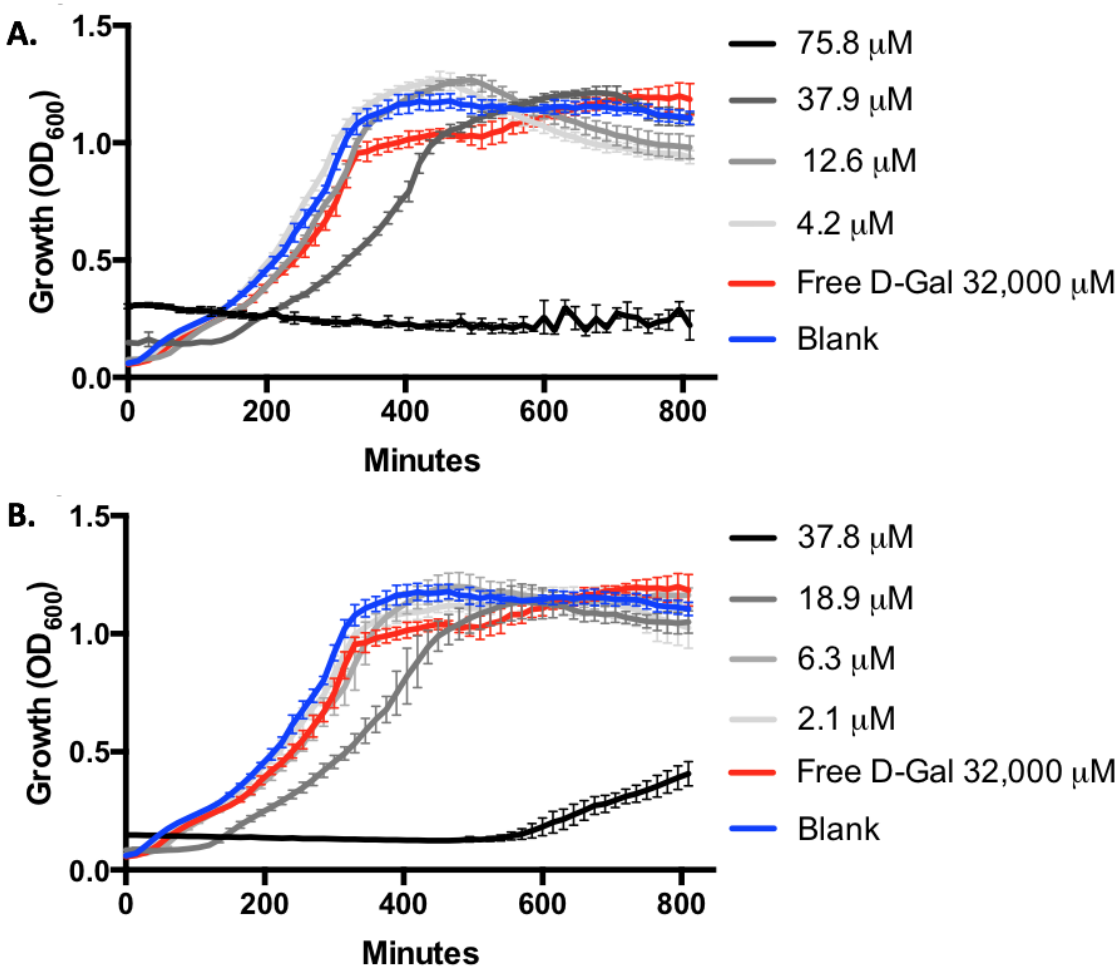

Figure 3. Evaluation of *P. aeruginosa* PAO1 growth by monitoring OD_{600} with 100%-D-galactose-surface-modified nanoparticles (A) and 50%-D-galactose-surface-modified nanoparticles (B). No significant growth inhibition is observed with 100%-modified Gal-NP at concentrations below 37.9 μM or with 50%-modified Gal-NP at concentrations below 18.9 μM. Growth inhibition was noted at concentrations two-fold higher than those employed in the biofilm inhibition assays (100% Gal-NP at 75.8 μM and 50% Gal-NP at 37.8 μM). Error bars represent standard deviation of triplicate analysis.

2.6 Evaluation of biofilm inhibition and morphology. We subsequently evaluated the inhibition of biofilm formation in the hyper-virulent isolate of *P. aeruginosa* PA14 by fluorescent confocal microscopy. Briefly, 24-h biofilms were prepared by inoculation of PA14-GFP [23] into Luria broth (LB) containing the appropriate treatments or controls. The resulting biofilm was then evaluated by fluorescent confocal microscopy. In this experiment, we observed clear changes in the overall biomass and average biofilm thickness of the Gal-NP-treated samples, consistent with our observations in the crystal violet assay. Additionally, in this experiment, we captured distinct changes in the morphology of the biofilm that are evident at sub-inhibitory concentrations. These observations further support the inhibition of cellular adhesion by D-galactose surface modified nanoparticles.

Within the 100%- and 50%-surface-modified samples of nanoparticles we observed the inhibition of biofilm formation based on evaluation of biofilm biomass and average biofilm thickness at concentrations above ~19.5 μM; however, effects on biofilm morphology were apparent at even lower concentrations (Figure 4). The slightly higher concentrations required to inhibit biofilm formation in the hypervirulent PA14 strain, compared with our crystal violet assay with PAO1, are consistent with previous studies of this bacteria [24,25]. In this assay, we observed no inhibition of biofilm formation by free D-galactose, even at concentrations of 48,000 μM (Figures 4 and 5). Visual inspection of the images collected (Figure 4 and Supporting Information) show that with increasing concentration of D-galactose-modified nanoparticles the biofilm begins to display increasing numbers of spaces within the biofilm structure (Figure 4, panel A vs. B vs. D).

This effect is consistent with the anticipated inhibition of cellular adhesion achieved by inhibiting the activity of LecA in the presence of Gal-modified nanoparticles.

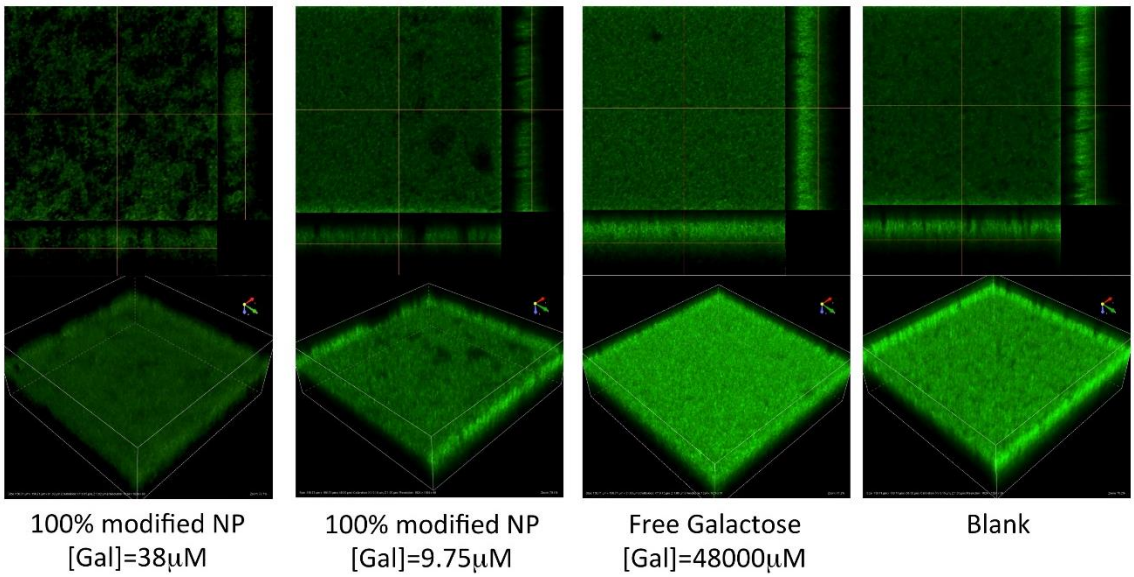

Figure 4. Fluorescent confocal microscopy evaluation of *P. aeruginosa* PA-14 biofilms. Samples treated with Gal-NP show inhibition of biofilm formation. The biofilm morphology at sub-inhibitory concentrations of Gal-NP (e.g. 100%-modified at 9.75 μM) shows evidence of anti-adhesive properties of Gal-NP, which increase with higher concentrations. For additional images see Supporting Information.

Quantification of the biomass and average biofilm thickness of the confocal images using the program Comstat2 shows dose-dependent inhibition of biofilm formation (Figures 5A and B). Most striking is the quantification of biofilm surface area as a function of volume. This calculation nominally provides a measure of the quantity/size of spaces within the biofilm structure. Consistent with the hypothesis that Gal-NP inhibit cellular adhesion without inhibiting growth/viability, we observe a dose-dependent increase in the biofilm surface area/volume (Figure 5C).

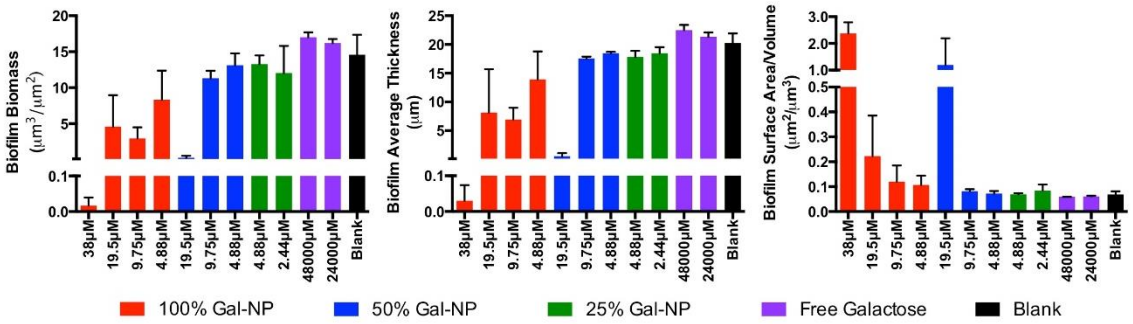

Figure 5. Quantification of (a) biofilm total biomass, (b) average biofilm thickness, and (c) biofilm surface area/volume from fluorescent confocal microscopy analysis. Images were analyzed using Comstat2 processing of duplicate analysis and are reported as means with error bars representing standard deviations.

3. Discussion

Recently, significant interest has been directed at the development of antivirulence strategies to combat infectious diseases. As these approaches do not directly impact viability or growth, a reduced selective pressure for resistance is anticipated. For the inhibition of biofilm formation, many antivirulence agents being developed focus on the inhibition of the quorum-sensing signaling pathways [14,24,26] or inhibition of bacterial adhesion [20,27,28]. Bacterial lectins are implicated in key roles in bacterial adhesion and biofilm formation, including the lectins LecA and LecB, which play a prominent role in *P. aeruginosa*. Here we report the development of the first LecA-targeted surface-modified polymeric nanoparticle. The particles prepared showed high avidity for LecA in the inhibition of hemagglutination, consistent with a beneficial effect of multivalent display of the lectin ligand on the particle surface. We observed greater than 100-fold enhancement in potency, compared with free D-galactose in the assay with 100%- and 50%-surface modified D-galactose nanoparticles. Further, we demonstrated potent

inhibition of *P. aeruginosa* biofilm formation in the presence of these surface-modified nanoparticles, demonstrating the anti-virulence potential of these novel inhibitors of the *P. aeruginosa* lectin LecA.

Previous studies have shown that LecA is cytotoxic [29] and has an important role in cellular adhesion and lung infection [17]. LecA is a homotetramer and displays specificity for galactose. Due to the high affinity of LecA for galactose, numerous multivalent and dendrimer structures have been developed as inhibitors of this protein [12,20,27,28]. The significant increase in LecA binding potency noted in these dendrimeric constructs was captured in the polymeric nanoparticles in this study, which were found to be potent inhibitors of LecA-induced hemagglutination and bacterial biofilm formation.

Notably, the assembly of nanoparticles as highly multivalent scaffolds for lectin binding avoids many of the synthetic challenges of dendrimer synthesis [30,31]. Accordingly, we anticipate that the application of polymeric nanoparticles to achieve the high lectin-binding potency observed with dendrimers, as demonstrated here, will serve as a powerful and useful complimentary approach for the inhibition of bacterial lectins and other cell-surface receptors. Self-assembly of sugar-modified di-block co-polymers using flash nanoprecipitation [19] further enables ready introduction of multiple different ligands to enable targeting multiple biological targets with a single nanoparticle construct, further enhancing biological activity.

Polymeric nanoparticles have been extensively studied in several medical technologies, especially in the area of drug delivery [11,32–37]. The advantages of improved pharmacokinetics and therapeutic properties, including mucus penetration [38],

continue to stimulate interest in the field. As demonstrated here, surface modification of the nanoparticle enables targeting of the constructs to the bacterial pathogens of interest, potentially enabling species-specific delivery of drugs, diagnostic reagents, or other small molecules.

4. Conclusion

In conclusion, polymeric nanoparticles synthetically modified to provide surface display of conjugated D-galactose bind to the *P. aeruginosa* lectin LecA with high potency. The benefit of high ligand valency to achieve high avidity lectin binding is efficiently realized in these constructs. Several of the polymeric nanoparticles were found to inhibit biofilm formation in a manner consistent with an antivirulence (anti-adhesion) mechanism of action, providing a new and powerful technology for species-specific inhibition of bacterial virulence.

Chapter 2

Synthesis of Tetra-Galactose Modified Polymers

The data that was acquired from the mono Galactose modified nanoparticles was very promising. As the active functionality contributing to the observed inhibition of *P. aeruginosa* biofilms is only a simple, polymer linked, naturally occurring sugar the observation of inhibition to the levels we observed is especially notable. In our studies we observed activity at relative concentrations of 38μM of Galactose on the nanoparticle surface contrasting observing no activity up to 38,000μM of free Galactose. Therefore, while the simple Galactose sugar is necessary for activity, it is not sufficient. In addition to the presence of Galactose it is critical that the sugar be localized onto the particle surface. Importantly, unmodified nanoparticles and Mannose modified particles show no inhibition of *P. aeruginosa* biofilm. The mono Galactose modified nanoparticles have a significant effect on the biofilm inhibition of *P. aeruginosa*. This was a great first step to making bacteria selective antibiotics.

The next step of this project is to make new and improved Galactose modified nanoparticles; however, the new nanoparticles will have more modified Galactose going from mono Galactose to multi-valent Galactose. The first target molecule was to make a di-valent Galactose molecule to essentially double the amount of sugars on the nanoparticles. While making this molecule, we figured out that we could quadruple the amount of sugars on the nanoparticles. This can be accomplished by using Cyanuric

Chloride and modifying it with one of the chlorines substituted with the polymer and the other two chlorines substituted with the di-valent galactose sugars that were made.

5. Results

5.1 Optimization of Mono-Boc diamine linker. The first step to making the tetra galactose modified polymer was to synthesize the mono-boc diamine linker that will be linked to lysine. A simple boc protecting mechanism turned out to be more challenging to selectively add one boc protecting group to a diamine substrate. First attempt was to do a 1:1 stoichiometry which should give mono-boc to the diamine. After looking at the H-NMR, the product ended up being bis-boc on the diamine which is not what was the goal. The reaction conditions were screened in order to optimize the reaction scheme to create the mono-boc diamine linker. Table 3 shows the reaction conditions that were screened.

Table 3.

Screened reaction conditions for the optimization of mono-boc diamine linker

Stoichiometry (Diamine : Boc)	Temperature	Solvent	Mono-boc	Yield
1:1	23˚C	DCM	No	0%
1:1	0˚C	DCM	No	0%
1:1	-40 ˚C	DCM	No	0%
1:1	-80 ˚C	DCM	No	0%
1:1	23˚C	Methanol	No	0%
1:1	23˚C	Ethyl Acetate	No	0%
1:0.9	23˚C	DCM	Yes	< 2%
1:0.75	23˚C	DCM	Yes	15%
1:0.4	23˚C	DCM	Yes	95%
1:0.1	23˚C	DCM	Yes	90%

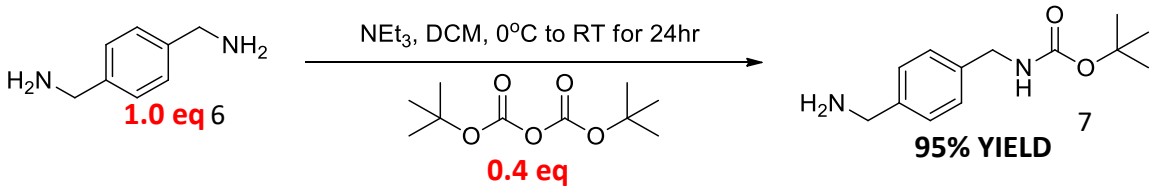

Scheme 2. Optimized mechanism of mono-boc protected diamine linker for galactose modified lysine.

The conformation of the product was done by analyzing the H-NMRs of the products. In figure 6 the left H-NMR is the bis-boc diamine confirmed by the integration of the boc protons at δ1.48 showing 18. The reaction conditions for that was a 1:1 ratio of diamine and boc. After screening the reaction conditions, ultimately the best conditions were decreasing the amount of boc used to 0.4 eq. After doing this change, the H-NMR confirmed that the reaction did indeed give mono-boc instead of bis-boc on the diamine. After purification the H-NMR shows the integration of 9 protons at δ1.46.

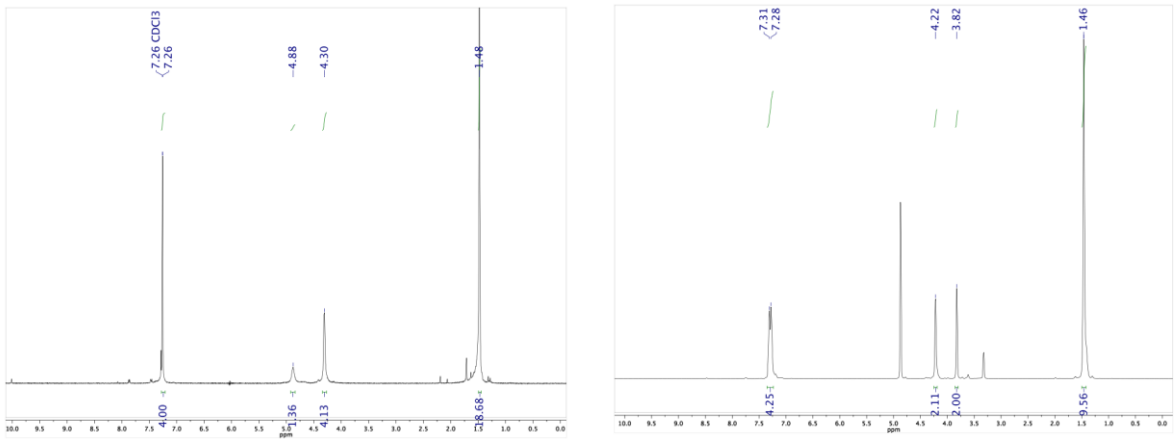

Figure 6. H-NMR comparison of bis-boc (Left) and H-NMR of mono-boc (7) (Right).

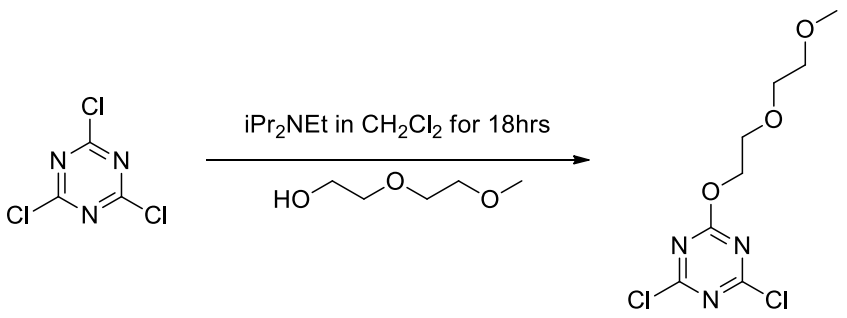

Scheme 3. Synthesis of TCT coupled to Diethylene Glycol Monomethyl Ether.

5.2 Confirmation of di-chlorotriazine PS-PEG. In order to test that the PS-PEG-OH 6.6kD was binding to TCT, we used Diethylene Glycol Monomethyl Ether as a template to see binding. Diethylene Glycol Monomethyl Ether is a much smaller PEG which allows us to interpret if we are getting modified TCT or not. In order to test this, knowing the what the starting material H-NMR and C-NMR was crucial. Diethylene Glycol Monomethyl Ether's H-NMR shifts are important because we wanted to see if it was binding to the TCT. Looking at the shift in starting material H-NMR and product H-NMR it is clear that the Diethylene Glycol Monomethyl Ether bound to something. As shown in Figure 7, the protons shifted higher following ChemDraw predictions.

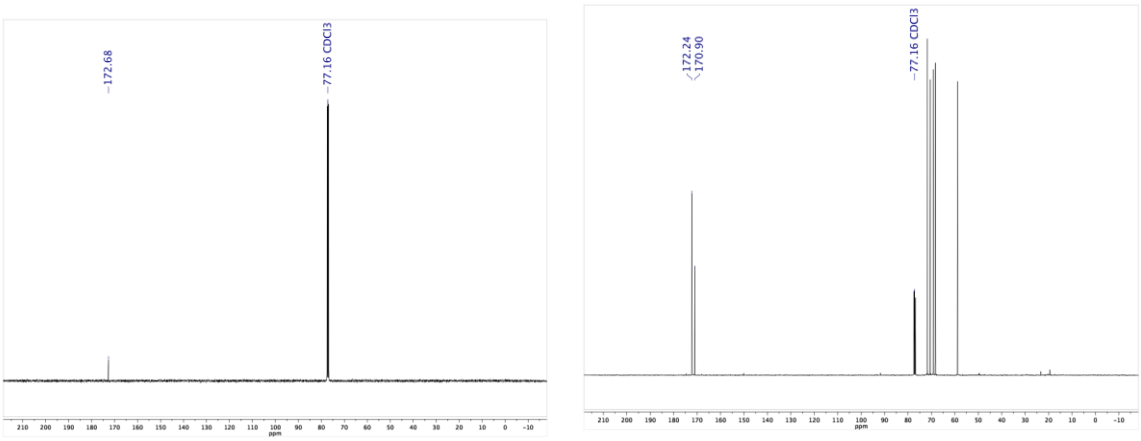

Figure 7. H-NMR of unreacted Diethylene Glycol Monomethyl Ether (Left), reacted Diethylene Glycol Monomethyl Ether with TCT (Right)

The next thing to check is if the Diethylene Glycol Monomethyl Ether is bound to TCT. In order to characterize this, C-NMR of the starting material of TCT and C-NMR of product are interpreted. The starting material TCT's C-NMR shows one peak at δ172 which are for the 3 carbons in TCT. When the C-NMR of product is looked at, there is 1 new peak that shows up at δ171. The new peak is lower and shorter telling us that Diethylene Glycol Monomethyl Ether was bound once to TCT.

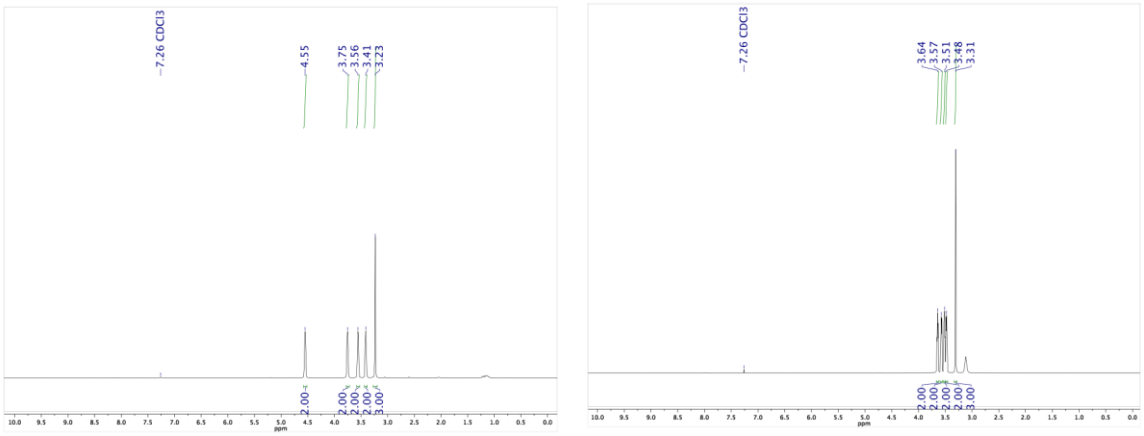

Figure 8. C-NMR comparison of unreacted TCT (Left) and Diethylene Glycol Monomethyl Ether reacted with TCT (Right)

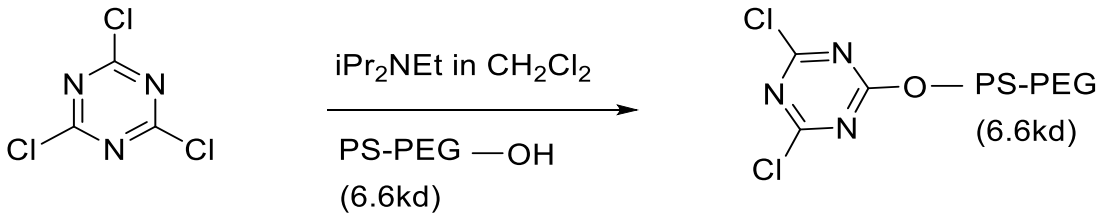

Scheme 4. Mechanism of addition of PS-PEG-OH (6.6kD) to TCT.

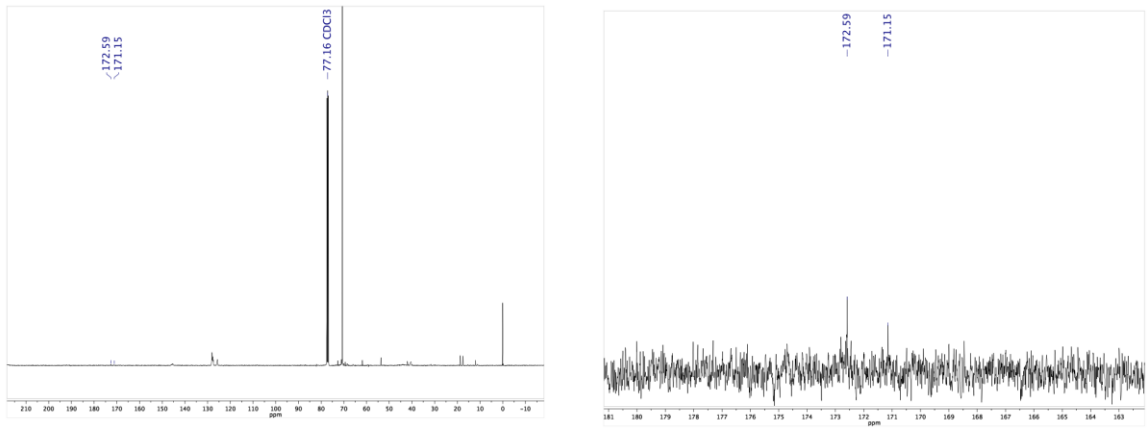

Figure 9. C-NMR of TCT reacted with PS-Peg-OH (6.6kD) confirmation compared to Scheme 3 C-NMR. Important peaks at δ172 and δ171.

5.3 Synthesis of tetra galactose-modified di-block co-polymer. In order to make the final product, the bis galactose lysine with the diamine linker needed to be added to the TCT at the other available sites of the TCT. After doing some research, in order to get both of the chorlines to leave and have our lysine added, the termperature needs to get to 80°C. The tricky part of this reaction was to get it to actually work. While on paper it seemed trivial, the execution was much complicated. It is not entirly known how polymers are position in solution, but increasing temperature could cause the polymer to rotatate around itself not allowing the lysine to bind to the polymer. We need heat to get the reacton to work so that needs to be done. The first attemped was to just stir and heat at 80°C for 2 day using an oil bath. This did not show any modification of the TCT with Lysine. We got it to temperature but still no reaction. The next condition we looked at was the stiring, maybe the stir bar on the plate is not stiring enough. We then used the sonicator at 80°C. This again did not change the outcome and there was still no modification of the TCT. The last attempt was two things that were changed. The first

thing that was changed was the equivilence of the lysine. Instead of doing just 2 equivilence of lysine, this was increased to 10 equivilence. The second change was to use the microwave. Thinking that the microwave will heat it from all around the reacting vs from the outside in like tradition oil baths. The microwave also decreases the time of the reaction turning a 2 day reaction into 2 hours. The reaction also only needed to be heated to 70°C with 100 power. This change in the reaction gave up product which was confirmed by MALDI show in Figure 10.

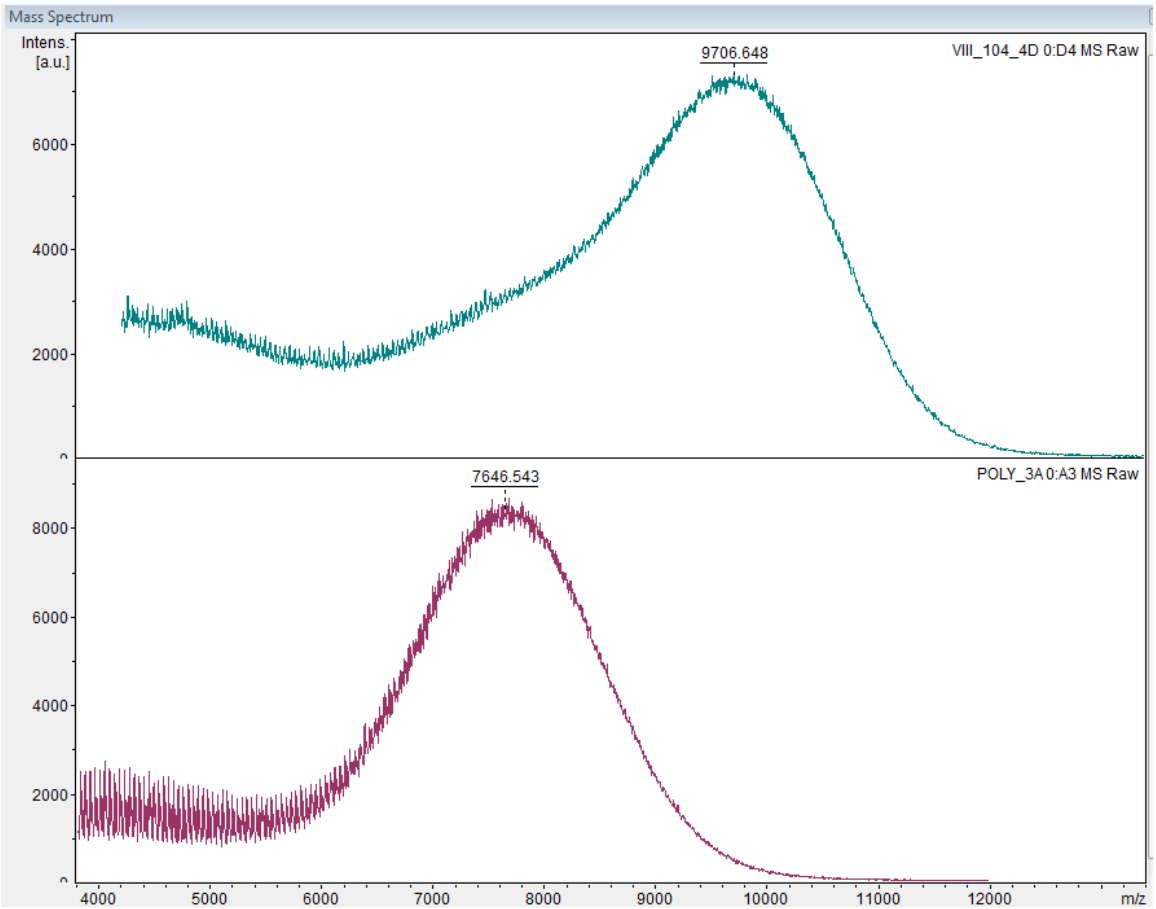

Figure 10. Maldi mass of product 13 in green and the starting material PS-PEG-OH (7.6 kD) in pink.

Instead of targeting a sugar with a carboxylic acid to couple to an amine-terminated polymer as before, a strategy that would employ a sugar with a free amine to couple to an electrophilic polymer reagent (Figure 3). In three steps from bis-Fmoc-Lys-OH (**8**), I can prepare multi-gram quantities of intermediate **9**. I envisioned coupling this intermediate, after liberation of the Boc-protected benzyl amine, to an electrophilic polymer species. My current approach involves using cyanuric chloride (TCT) which is a chlorinated derivative of 1,3,5-triazine that has been linked the polystyrene peg to one chlorine position (**12**). If the remaining two electrophilic sites on the heteroaromatic linker can be engaged in reaction with the sugar-containing amine then two lysines that are double modified with galactose would be incorporated to enable the assembly of a tetra-modified galactose polymer. This can be done by doing the boc deprotection of the lysine with the di-galactoce modified sugars (10) and reacting this with (12) in the microwave for 2 hours at 70°C with 100 power. Product (13) was confirmed by MALDI.

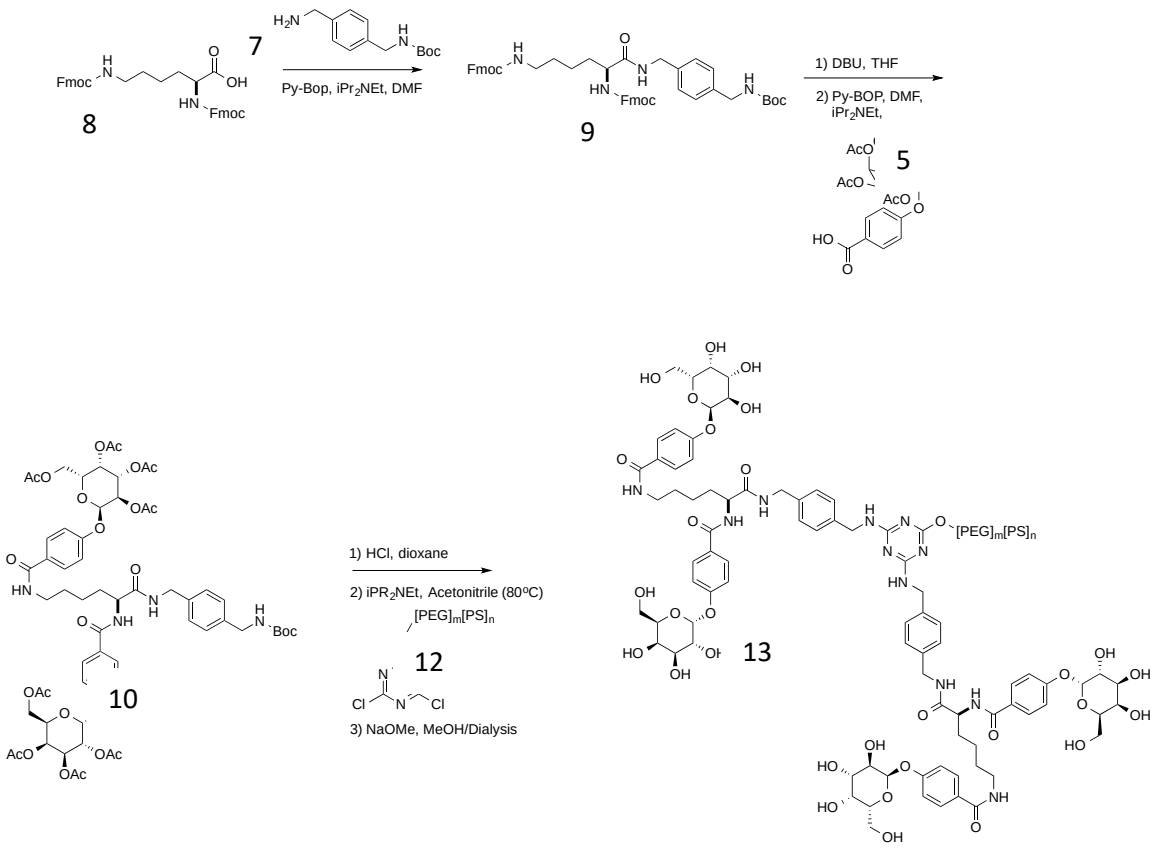

Scheme 5. Synthesis of tetra Galactose-modified polymer for nanoparticle assembly.

Chapter 3

Supporting Information

6. Materials and Methods

6.1 General experimental. Unless otherwise noted, all reactions were performed in flame-dried glassware under an atmosphere of nitrogen or argon using dried reagents and solvents. All chemicals were purchased from commercial vendors and used without further purification. Anhydrous solvents were purchased from commercial vendors.

Flash chromatography was performed using standard grade silica gel 60 230-400 mesh from SORBENT Technologies or using a Biotage Flash Purification system equipped with Biotage SNAP columns. All purifications were performed using gradients of mixtures of ethyl acetate and hexanes. Analytical thin-layer chromatography was carried out using Silica G TLC plates, 200 μm with UV_{254} fluorescent indicator (SORBENT Technologies), and visualization was performed by staining and/or absorbance of UV light.

NMR spectra for small molecules were recorded using a Varian Mercury Plus spectrometer (400 MHz for ^{1}H-NMR; 101 MHz for ^{13}C-NMR). Chemical shifts are reported in parts per million (ppm) and were calibrated according to residual protonated solvent. Mass spectroscopy data was collected using an Agilent 1100-Series LC/MSD Trap LC-MS or a Micromass Quattromicro with a Waters 2795 Separations Module LC-MS with acetonitrile containing 0.1% formic acid as the mobile phase in positive ionization mode. Small molecule purity was determined on an Agilent 1100 series

equipped with a Phenomenex Kinetex 2.6 µm C18-UPLC column using a gradient of water to acetonitrile with 0.1% TFA.

All final compounds were evaluated to be of greater than 90% purity by analysis of ^{1}H-NMR, ^{13}C-NMR, and/or analytical HPLC.

6.2 Synthesis of D-galactose-modified polymers. (2*S*,3*R*,4*S*,5*S*,6*R*)-6-(acetoxymethyl)tetrahydro-2*H*-pyran-2,3,4,5-tetrayl tetraacetate, 2. D-galactose (5.00 g, 27.75 mmol) was dissolved in acetic acid (185 mL, 0.15 M) at room temperature. Acetyl bromide (16.40 mL, 222.02 mml) was added and the mixture was allowed to stir for 1 hour. The resulting solution was washed with toluene (2x, 40 mL), dried over sodium sulfate, and concentrated to dryness. The residue was purified by flash chromatography using a gradient of hexanes to EtOAc to provide (2*S*,3*R*,4*S*,5*S*,6*R*)-6-(acetoxymethyl) tetrahydro-2*H*-pyran-2,3,4,5-tetrayl tetraacetate. Characterization data was consistent with a commercial sample of this compound.

(2*R*,3*S*,4*S*,5*R*,6*S*)-2-(acetoxymethyl)-6-(4-((benzyloxy)carbonyl)phenoxy)tetrahydro-2*H*-pyran-3,4,5-triyl triacetate, 4. (2*S*,3*R*,4*S*,5*S*,6*R*)-6-(acetoxymethyl)tetrahydro-2*H*-pyran-2,3,4,5-tetrayl tetraacetate, **2** (2 g, 5.12 mmol) was dissolved in dichloromethane (10 mL, 0.5 M) at room temperature. Hydrobromic acid (33% in AcOH, 1.485 mL) and acetic acid (3.015 mL, 1.14 M) were added and the mixture was allowed to stir. After 30 minutes, the solution was diluted with 50 mL of DCM, washed with sodium bicarbonate, dried with sodium sulfate, and concentrated to dryness. The residue (2 g) was re-dissolved in DCM (30 mL, 1.5 M) and treated with benzyl-4-hydroxybenzoate, **3** (2.34 g, 10.03 mmol), tetrabutylammonium hydrogensulfate (1.74 mg, 5.12 mmol), and 0.5 M sodium hydroxide (10 mL, 0.5 M).

The biphasic mixture was allowed to stir overnight at room temperature, was diluted with DCM and acidified with 1M HCl, extracted with DCM (3 x 50mL), dried over Na_2SO_4, and concentrated to dryness. The residue was purified by flash chromatography using a gradient of hexanes to EtOAc to provide (2*R*,3*S*,4*S*,5*R*,6*S*)-2- (acetoxymethyl)-6-(4-((benzyloxy)carbonyl)phenoxy) tetrahydro-2*H*-pyran-3,4,5-triyl triacetate, **4** (1.006 g, 1.848 mmol, 40.76%). ^{1}H NMR (400 MHz, $CDCl_3$) δ^1H NMR (400 MHz, $CDCl_3$) δ 7.96 (d, *J* = 8.9 Hz, 2H), 7.40–7.22 (m, 5H), 6.95 (d, *J* = 8.4 Hz, 2H), 5.48–5.37 (m, 2H), 5.27 (s, 2H), 5.11–5.01 (m, 2H), 4.20–3.95 (m, 3H), 2.11 (s, 3H), 1.98 (s, 6H), 1.94 (s, 3H). ^{13}C NMR (101 MHz, $CDCl_3$) δ 170.44, 170.30, 170.19, 169.44, 165.88, 160.46, 136.19, 131.84, 128.72, 128.37, 128.25, 125.14, 116.30, 98.93, 71.39, 70.84, 68.59, 66.93, 66.76, 66.76, 61.50, 20.82, 20.79, 20.76, 20.69, 0.12. ESI-MS: predicted for $C_{28}H_{31}O_{12}$ $[M+H]^+$ 559.544, observed, 559.569.

4-(((2*S*,3*R*,4*S*,5*S*,6*R*)-3,4,5-triacetoxy-6-(acetoxymethyl)tetrahydro-2*H*-pyran-2-yl)oxy)benzoic acid, 5. (2*R*,3*S*,4*S*,5*R*,6*S*)-2-(acetoxymethyl)-6-(4-((benzyloxy)carbonyl)phenoxy)tetrahydro-2*H*- pyran-3,4,5-triyl triacetate, **4** (0.719 g, 1.320 mmol) was dissolved in methanol (6.6 mL, 0.2 M) and palladium on carbon (10%, 16 mg, 0.1 mmol) was added to the reaction flask at room temperature. Hydrogen was added via balloon and the reaction was stirred overnight at room temperature. The residue was separated by vacuum filtration washing with methanol to yield 4-(((2*S*,3*R*,4*S*,5*S*,6*R*)-2,3,4,5-tetrahydroxy-6-(hydroxymethyl)tetrahydro-2*H*-pyran-2-yl) methoxy)benzoic acid, **5** (571.2 mg, 1.219 mmol, 61.85%). ^{1}H NMR (400 MHz, $CDCl_3$) δ 8.05 (d, *J* = 8.3 Hz, 2H), 7.03 (d, *J* = 8.3 Hz, 2H), 5.57–5.43 (m, 2H), 5.20–5.07 (d, *J* = 51.1 Hz, 2H), 4.28–4.06 (d, *J* = 84.7 Hz, 3H), 2.19 (s, 3H), 2.06 (s, 6H), 2.02 (s, 3H). ^{13}C NMR (101

MHz, $CDCl_3$) δ 171.98, 171.91, 171.38, 171.22, 161.55, 132.97, 132.72, 117.02, 115.98, 99.36, 72.27, 72.16, 70.02, 68.67, 62.60, 49.00, 24.74, 20.69, 20.60, 20.54, 20.50, 20.49, 13.93. ESI-MS: predicted for $C_{21}H_{24}O_{12}Na$ $[M+Na]^+$ 491.401, observed, 491.477.

PS-*b*-PEG-Galactose, 1. To a room temperature solution of 4-(((2*S*,3*R*,4*S*,5*S*,6*R*)-2,3,4,5-tetrahydroxy-6-(hydroxymethyl)tetrahydro-2*H*-pyran-2-yl) methoxy)benzoic acid, **5** (20.5 mg, 0.068 mmol) in DMF (340uL) was added (Benzotriazol-1-yloxy)tris(dimethylamino)phosphonium hexafluorophosphate (30.1 mg, 0.068 mmol) and the mixture was allowed to stir for 5 minutes before the addition of PS-*b*-PEG-NH_2 (150 mg, 0.023 mmol, 6.6 kD, prepared from PS-*b*-PEG-OH as previously described [18]). The resulting solution was stirred at room temperature overnight. The reaction was quenched by the addition of water (1 mL) and EtOH (1 mL), and loaded into a 3.5 kD MWCO dialysis cassette (Pierce™ Slide-A-Lyzer™ G2, Thermo Scientific). The mixture was dialyzed into water for 12 h, at which time the dialysis cassette was transferred to a fresh solution of water and further dialyzed for an additional 12 h. After dialysis, the retained solution was lyopholyzed to provide PS-*b*-PEG-galactose, 1, as a white powder (153.6 mg, quantitative). The product was characterized by MALDI-MS (Bruker MicroFlex LFR MALDI-TOF) in positive linear detection mode using a matrix of dithranol:polymer of 1:1 evaporated from DCM onto a polished steel target. Collected spectra were analyzed with the Flex Analysis software (Bruker); the unmodified PS-*b*-PEG-NH_2 was evaluated in the same manner as a standard. The observed m/z for PS-*b*-PEG-NH_2 was 6212.07, and the observed m/z for PS-*b*-PEG-galactose was 6501.40, consistent with complete polymer modification (anticipated Δ m/z for polymer modification = 282.24).

6.3 Nanoparticle assembly. Nanoparticles with defined levels of surface modification were prepared through flash nanoprecipitation (FNP) as previously described [18,19,39]. Briefly, PS, vitamin E (VitE), PS-*b*-PEG, PS-*b*-PEG-galactose, and/or PS-*b*-PEG-mannose were dissolved at defined compositions in THF and rapidly micromixed with an equivalent volume of water within a confined impingement jet mixer, manufactured using HDPE (The Inventors Shop, Cinnaminson, NJ, USA), following the specifications provided [40], and diluted tenfold in a water collection bath. Particles with 0–100%-surface-modification of galactose or mannose were prepared using defined combinations of PS-*b*-PEG/PS-*b*-PEG-galactose or PS-*b*-PEG-mannose. Vitamin E was used as the core bulking material in all NP formulations. Particle sizes were assessed with dynamic light scattering analysis (90Plus Particle Size Analyzer, Brookhaven Instruments Corporation). Size distributions were determined with backscattering measurements from 658-nm illumination and displayed as intensity-weighted distributions; 'particle diameter' is the hydrodynamic diameter as calculated by DLS based on the Stokes Einstein equation using instrumental software. The composition of particles formed and particle size characterization data is provided in Table 1.

6.4 Hemagglutination assay. The LecA-induced hemagglutination assay was performed as reported with modifications [20]. LecA (PA-IL) was purchased from Sigma-Aldrich and used as received. Rabbit red blood cells (Innovative Research) at 100% were washed three times with 150 mM NaCl solution then diluted to 5% with NaCl (150 nM) solution. A hemocytometer was used to count the number of red blood cells that were in red blood cell solution and solutions were normalized to 2.94 x 10^{14} cells/mL. To find the minimal full hemagglutination inhibition concentration for LecA, a

serial dilution was performed from a stock solution of 1 mg/ml LecA. Briefly, LecA (15 µl) was diluted into Tris buffer (Tris 20 µM, NaCl 100 mM, $CaCl_2$ 100 µM, pH = 7.5, 35 µl) in 96-well microtiter V-bottom plates and was subjected to a two-fold serial dilution. Normalized 5% blood solution (10µl) was added to each well and incubated for 30 minutes at room temperature. After incubation, the plate was centrifuged for 1 minute at low rpm. The minimum full hemagglutination inhibition for LecA was found to be 1.2 µg/ml. Further analysis of inhibition of LecA-induced hemagglutination was performed with LecA at 4xHU (4.8 µg/ml). Briefly, 25 µl of each nanoparticle formulation was subjected to a two-fold serial dilution in Tris buffer and LecA was added to a final concentration of 4xHU. The plate was then incubated for 2 hours at room temperature. After incubation, normalized 5% blood solution (10 µl) was added. The plate was then incubated for 30 minutes at room temperature and then centrifuged for 1 minute at low rpm before analysis.

6.5 Crystal violet biofilm inhibition assay. The effect of inhibitors on static biofilm formation was evaluated using the crystal violet staining method with *P. aeruginosa* strain PAO1 [25] following the established procedure [41]. Briefly, overnight cultures of *P. aeruginosa* PAO1 were diluted 1:100 into fresh LB media. Compounds were added at the indicated concentrations in a 96-well microplate before static incubation at 37 °C for 24 hours. After incubation, the plates were thoroughly rinsed to remove planktonic cells and the adherent cells were quantified by staining with crystal violet and measurement of A_{550}. The assay was performed with five replicates for each compound concentration. After exclusion of the highest and lowest absorbance readings the remaining triplicate readings were described as means with error bars representing standard deviations.

6.6 Growth inhibition assay. The effect of nanoparticles on bacterial growth was evaluated with *P. aeruginosa* strain PAO1 [25]. Overnight cultures of *P. aeruginosa* PAO1 were diluted 1:100 into fresh LB media. Nanoparticle formulations/compounds were added at the indicated concentrations in a 96-well microplate. The plate was placed in a Molecular Devices SpectraMax i3x incubating plate reader set at 37 °C with shaking. Measurement of A_{600} was recorded every 15 minutes for the duration of the experiment. Readings are reported as means with error bars representing the standard deviations of triplicate analyses.

6.7 Fluorescent confocal microscopy. The effect of inhibitors on static biofilm formation was evaluated by confocal fluorescence microscopy with *P. aeruginosa* strain PA14 [25] following the established procedure [42]. Briefly, overnight cultures of PA14-GFP [23] were diluted 1:100 into the designated media. Compounds were added at the indicated concentrations in 96-well microplates with optical grade glass bottoms (Corning) before static incubation at 37 °C for 24 hours. After incubation, the samples were imaged on a Nikon Eclipse TI confocal microscope equipped with a 10X lens. Images were acquired from a central point in each well of the microplate. Each compound concentration was evaluated in duplicate. Image stacks were analyzed using Comstat2 [43, 44].

6.8. Synthesis of Tetra-Galactose Modified Polymers.

Mono-Boc Diamine 7. p-Xylyldiamine (0.200 g, 1.468 mmol) in DCM at 0°C. Triethylamine (0.500 mL, 3.5232 mmol) was added to cold solution. Next, a separate solution of Di-tert-butyl pyrocarbonate (0.1282 g, 0.5873 mmol) in DCM was added to

the first solution. This reaction was stired overnight (18hrs) to room temperature (23°C). The reaction was converted in vacuum and redissolved in DCM (30mL) washed with bicarb, brine, dryed, concentrated. **7** (0.1318 g, 0.5577 mmol, 95%)

Bis-Fmoc Lysine Mono-Boc Linker 9. To a solution of Bis-Fmoc-L-lysine (2.499 g, 4.23 mmol) and Mono-Boc Diamine **7** in DMF, N,N-diisopropylethylamine (3.55 mL, 20.30 mmol) and (Benzotriazol-1-yloxy) tripyrrolidinophosphonium hexafluorophosphate (2.64 g, 5.07 mmol) were added and reaction ran for 4 hours. Reaction was crashed out with water, the white solids were filtered, the white solids were then treated with Methanol and stirred overnight. Ten white solids were filtered out and were kept for further use. **9** (1.8276 g, 2.259 mmol, 53.5%)

Bis-Galactose Lysine Mono-Boc Linker 10. To a solution of Bis-Fmoc Lysine Mono-Boc Linker **9** (0.200 g, 0.2472 mmol) in DMF, 1,8-Diazabicyclo[5.4.0]undec-7-ene (0.369 mL, 2.472 mmol) was added. This reaction was stirred at room temperature (23°C) for 30 minutes. Once done, the reaction was treated with 24 mL of Diethyl Ether and stirred for 5 minutes then placed into the freezer for 30 minutes. The supernatant was removed and the solids were concentrated and used crude (Lysine Mono-Boc Linker) without further purification. The crude product (0.2472 mmol) was made into a solution with DMF and Modified D-Galactose **4** (0.2895 g, 0.6180 mmol) at room temperature (23°C). To this solution, N,N-diisopropylethylamine (0.2153 mL, 1.236 mmol) and (Benzotriazol-1-yloxy) tripyrrolidinophosphonium hexafluorophosphate (0.3216 g, 0.6180 mmol) were added and stirred for 4 hours at room temperature (23°C). Once done, the reaction was quenched with water (50 mL) and vacuum filtered. The white solids were extracted and concentrated to yield product **10** (0.292 g, 0.231 mmol, 93.4%)

Di-Chlorotriazine PS-PEG (6.6 kD) 12. To a solution of PS-PEG-OH (6.6 kD) (0.1037 g, 0.01364 mmol) in DCM, Trichorotriazine (0.0503 g, 0.2729 mmol) and N,N-diisopropylethylamine (0.006 mL, 0.03411 mmol) were added. The reaction ran for 48 hours at room temperature (23°C) and mixed by sonication. Rotavaped to dryness and crashed out product with Diethyl Ether. Solids were filtered out to produce **12** (0.0876 g, 0.01296 mmol, 95%)

Tetra-Galactose Modified Polymer 13. To a solution of **10** (0.1726 g, 0.1364 mmol) in DCM, Hydrogen chloride, 4M in 1,4-dioxane (682 µL,) was added and the reaction was run overnight at room temperature (23°C). The reaction was concentrated giving product Bis-Galactose Lysine linker and used crude without any further purification. The next step was to make a solution of previous product of Bis-Galactose Lysine linker (crude, 0.01364 mmol) and Di-Chlorotriazine PS-PEG (6.6 kD) **12** (0.08766 g, 0.01296 mmol) in DCM. To this solution, N,N-diisopropylethylamine (0.0010 mL, 0.05456 mmol) was added to the solution. This reaction was run at 70°C for 1 hour in the Microwave to produce product **13.**

6.9 H-NMR and C-NMR of Intermediates and Product

H-NMR of intermediate 9

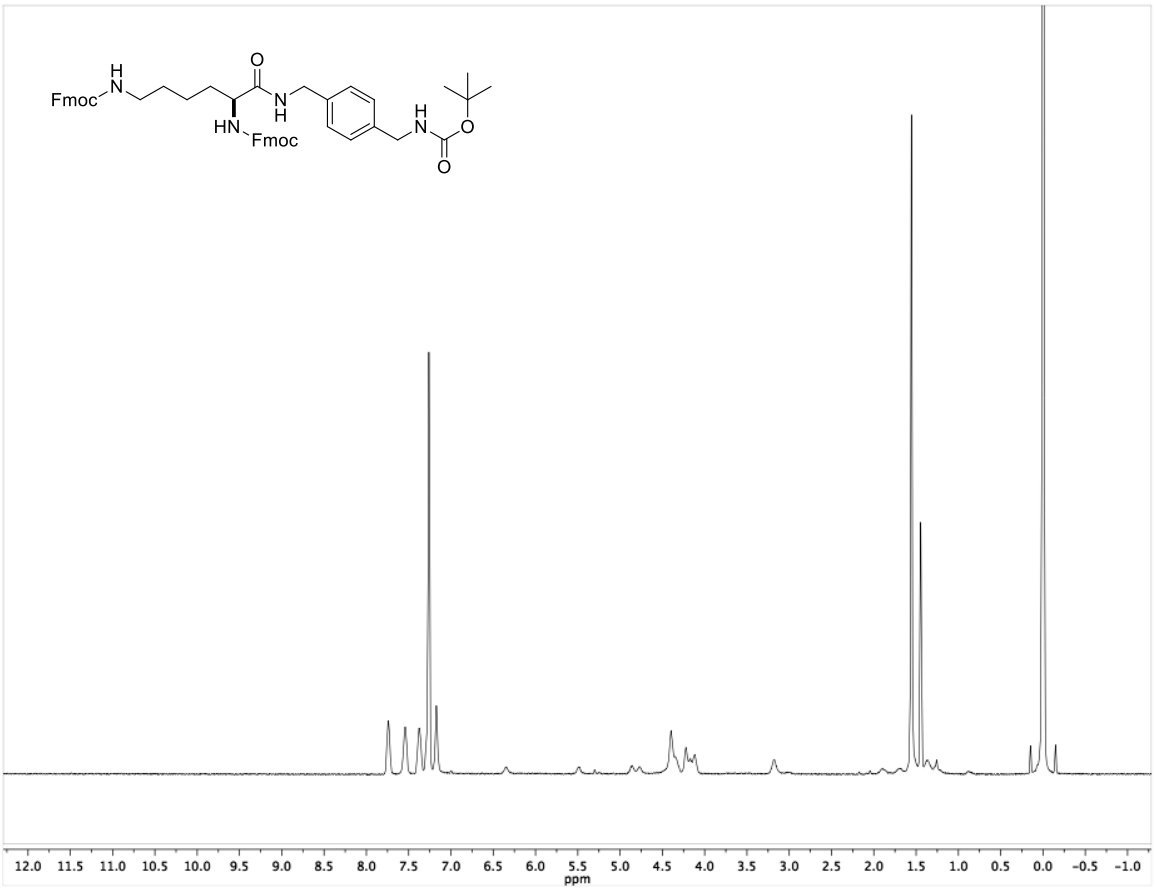

H-NMR of intermediate Fmoc Deprotection of intermediate 9

H-NMR of intermediate 10

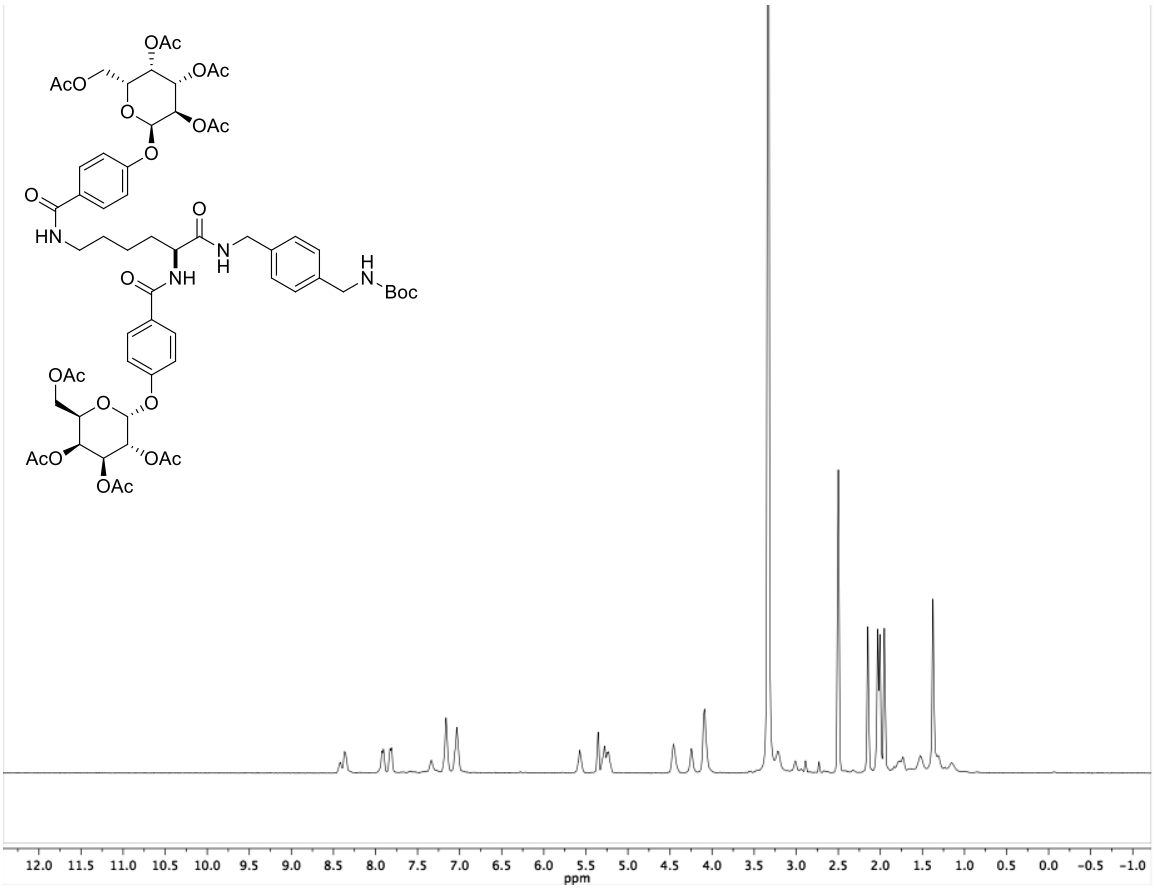

H-NMR of intermediate 12

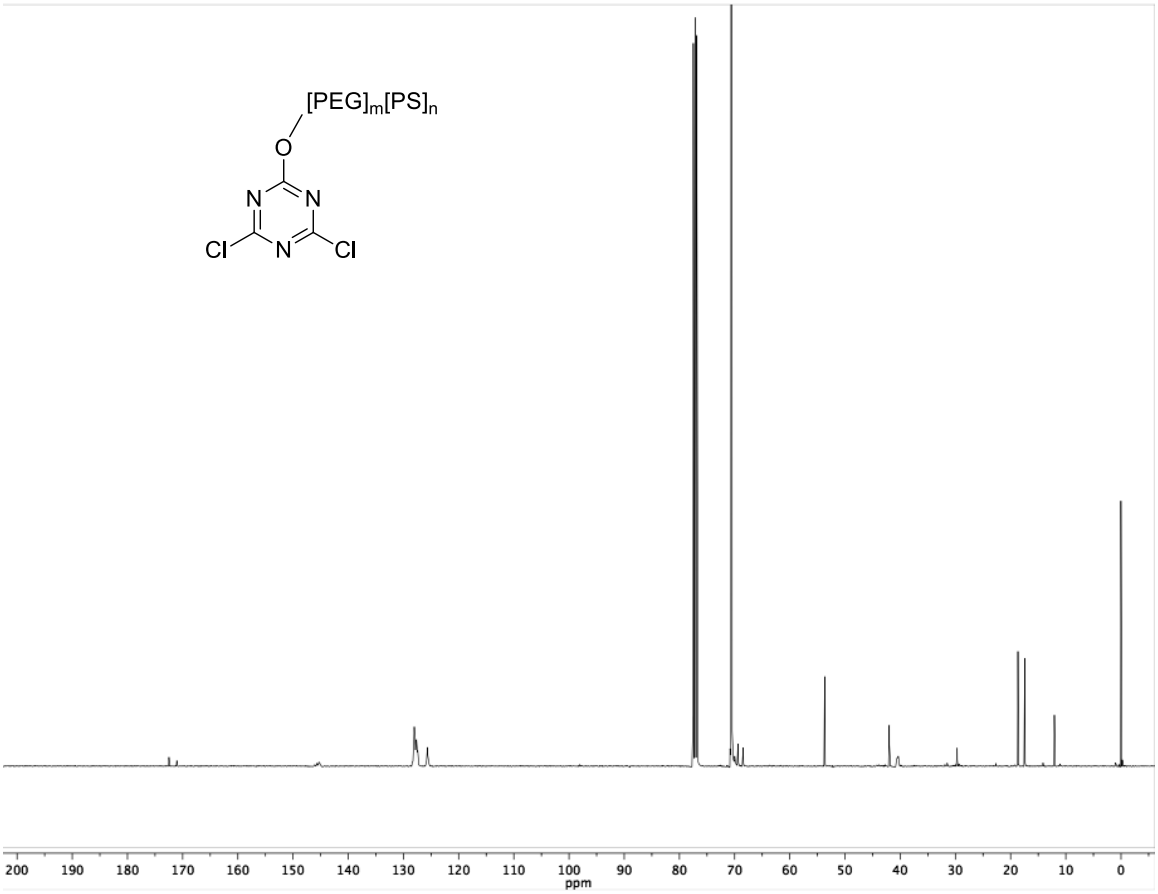

H-NMR of intermediate 13

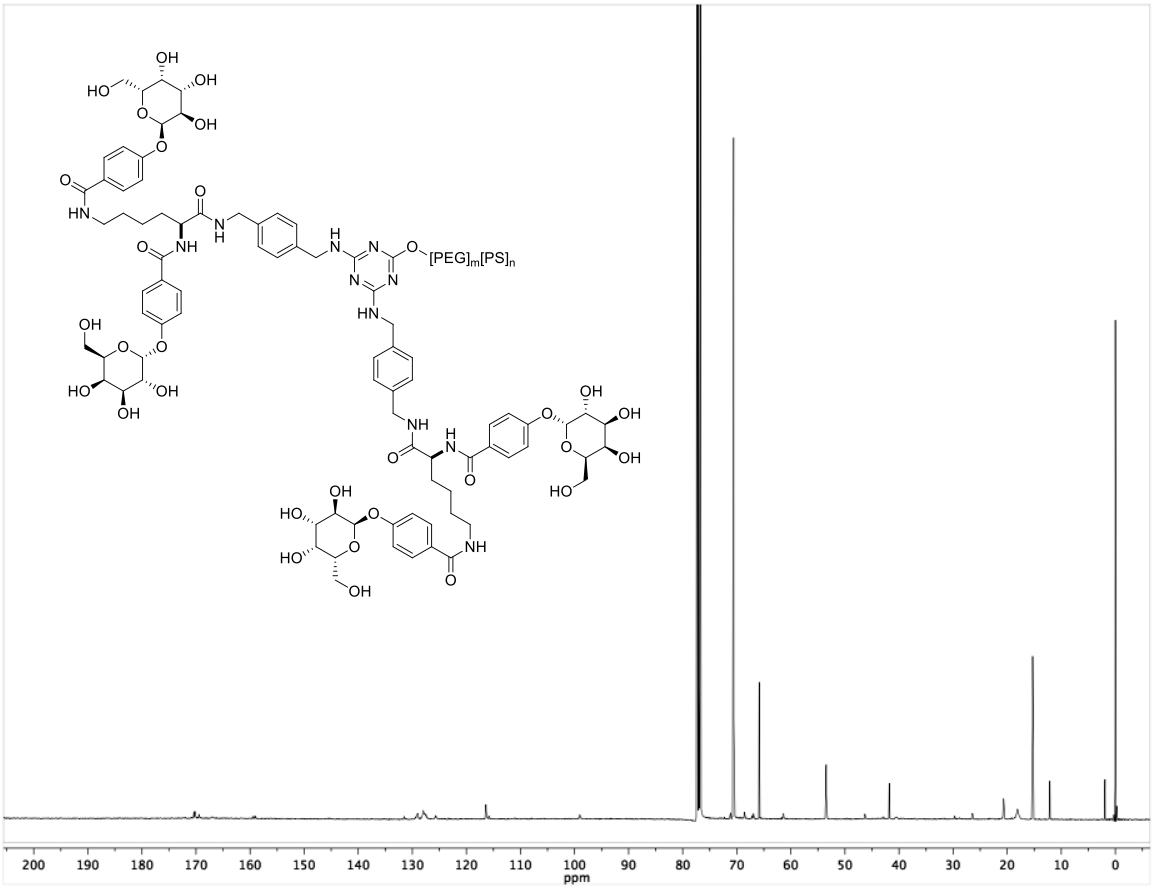

References

1. Fischbach, M.A.; Walsh, C.T. Antibiotics for emerging pathogens. *Science* **2009**, 325, 1089–1093.
2. Hirsch, E.B.; Tam, V.H. Impact of multidrug-resistant Pseudomonas aeruginosainfection on patient outcomes. *Expert Rev. Pharmacoeconom. Outcomes Res.* **2010**, *10*, 441–451.
3. Brown, E.D.; Wright, G.D. Antibacterial drug discovery in the resistance era. *Nature* **2016**, *529*, 336–343.
4. Sun, H.-Y. Pneumonia Due to Pseudomonas aeruginosa. *Chest* **2011**, *139*, 1172.
5. Wright, G.D. The antibiotic resistome: The nexus of chemical and genetic diversity. *Nat. Rev. Microbiol.* **2007**, *5*, 175–186.
6. Lister, P.D.; Wolter, D.J.; Hanson, N.D. Antibacterial-resistant *Pseudomonas aeruginosa*: Clinical impact and complex regulation of chromosomally encoded resistance mechanisms. *Clin. Microbiol. Rev.* **2009**, *22*, 582–610.
7. Centers for Disease Control and Prevention. *Antibiotic Resistance Threats in the United States*; US Department of Health and Human Services: Washington, DC, USA, 2013. Available online: https://www.cdc.gov/drugresistance/biggest_threats.html (accessed on 4 September 2019).
8. Oliver, A. High frequency of hypermutable *Pseudomonas aeruginosa* in cystic fibrosis lung infection. *Science* **2000**, *288*, 1251–1253.
9. Deretic, V.; Schurr, M.J.; Boucher, J.C.; Martin, D.W. Conversion of *Pseudomonas aeruginosa* to mucoidy in cystic fibrosis: Environmental stress and regulation of bacterial virulence by alternative sigma factors. *J. Bacteriol.* **1994**, *176*, 2773–2780.
10. Wagner, S.; Sommer, R.; Hinsberger, S.; Lu, C.; Hartmann, R.W.; Empting, M.; Titz, A. Novel strategies for the treatment of *Pseudomonas aeruginosa* infections. *J. Med. Chem.* **2016**, *59*, 5929–5969.
11. Hadinoto, K.; Cheow, W.S. Nano-antibiotics in chronic lung infection therapy against Pseudomonas aeruginosa. *Colloids Surf. B Biointerf.* **2014**, *116*, 772–785.
12. Grishin, A.V.; Krivozubov, M.S.; Karyagina, A.S.; Gintsburg, A.L. Pseudomonas *Aeruginosa Lectins* as targets for novel antibacterials. *Acta Nat.* **2015**, *7*, 29–41.
13. Winzer, K.; Falconer, C.; Garber, N.C.; Diggle, S.P. The *Pseudomonas aeruginosa* lectins PA-IL and PA-IIL are controlled by quorum sensing and by RpoS. *J. Bacteriol.* **2000**, *182*, 6401–6411.
14. Mattmann, M.E.; Blackwell, H.E. Small molecules that modulate quorum sensing and control virulence in *Pseudomonas aeruginosa*. *J. Org. Chem.* **2010**, *75*, 6737–6746.
15. Tielker, D.; Hacker, S.; Loris, R.; Strathmann, M.; Wingender, J.; Wilhelm, S.; Rosenau, F.; Jaeger, K.-E. *Pseudomonas aeruginosa* lectin LecB is located in the outer membrane and is involved in biofilm formation. *Microbiology* **2005**, *151*, 1313–1323.
16. Imberty, A.; Wimmerova, M.; Mitchell, E.P. Structures of the lectins from Pseudomonas aeruginosa: Insights into the molecular basis for host glycan recognition. *Microbes Infect.* **2004**, *6*, 221–228.

17. Chemani, C.; Imberty, A.; de Bentzmann, S.; Pierre, M.; Wimmerova, M.; Guery, B.P.; Faure, K. Role of lecA and lecB lectins in *Pseudomonas aeruginosa*-induced lung injury and effect of carbohydrate ligands. *Infect. Immun.* **2009**, *77*, 2065–2075.
18. Lu, H.D.; Yang, S.S.; Wilson, B.K.; McManus, S.A.; Chen, C.V.H.H.; Prud'homme, R.K. Nanoparticle targeting of gram-positive and gram-negative bacteria for magnetic-based separations of bacterial pathogens. *Appl. Nanosci.* **2017**, *7*, 83–93.
19. D'addio, S.M.; Prud'homme, R.K. Controlling drug nanoparticle formation by rapid precipitation. *Adv. Drug Deliv. Rev.* **2011**, *63*, 417–426.
20. Cecioni, S.; Imberty, A.; Vidal, S. Glycomimetics versus multivalent glycoconjugates for the design of high affinity lectin ligands. *Chem. Rev.* **2015**, *115*, 525–561.
21. Peeters, E.; Nelis, H.J.; Coenye, T. Comparison of multiple methods for quantification of microbial biofilms grown in microtiter plates. *J. Microbiol. Methods* **2008**, *72*, 157–165.
22. Coenye, T.; Nelis, H.J. In vitro and in vivo model systems to study microbial biofilm formation. *J. Microbiol. Methods* **2010**, *83*, 89–105.
23. Drescher, K.; Shen, Y.; Bassler, B.L. Biofilm streamers cause catastrophic disruption of flow with consequences for environmental and medical systems. *Proc. Nat. Acad. Sci. USA* **2013**, *110*, 4345–4350.
24. O'Brien, K.T.; Noto, J.G.; Nichols-O'Neill, L.; Perez, L.J. Potent irreversible inhibitors of LasR quorum sensing in *Pseudomonas aeruginosa*. *ACS Med. Chem. Lett.* **2015**, *6*, 162–167.
25. Rahme, L.G.; Stevens, E.J.; Wolfort, S.F.; Shao, J.; Tompkins, R.G.; Ausubel, F.M. Common virulence factors for bacterial pathogenicity in plants and animals. *Science* **1995**, *268*, 1899–1902.
26. Capilato, J.N.; Philippi, S.V.; Reardon, T.; McConnell, A.; Oliver, D.C.; Warren, A.; Adams, J.; Wu, C.; Perez, L.J. Development of a novel series of non-natural triaryl agonists and antagonists of the Pseudomonas aeruginosa LasR quorum sensing receptor. *Bioorg. Med. Chem.* **2017**, *25*, 153–165.
27. Titz, A. Carbohydrate-based anti-virulence compounds against chronic *Pseudomonas aeruginosa* Infections with a focus on small molecules. *Top. Med. Chem.* **2014**, *12*, 169–186.
28. Imberty, A.; Chabre, Y.M.; Roy, R. Glycomimetics and glycodendrimers as high affinity microbial anti-adhesins. *Chem. Eur. J.* **2008**, *14*, 7490–7499.
29. Bajolet-Laudinat, O.; Girod-de Bentzmann, S.; Tournier, J.M.; Madoulet, C.; Plotkowski, M.C.; Chippaux, C.; Puchelle, E. Cytotoxicity of *Pseudomonas aeruginosa* internal lectin PA-I to respiratory epithelial cells in primary culture. *Infect. Immun.* **1994**, *62*, 4481–4487.
30. Carlmark, A.; Hawker, C.; Hult, A.; Malkoch, M. New methodologies in the construction of dendritic materials. *Chem. Soc. Rev.* **2009**, *38*, 352–362.
31. Grayson, S.M.; Frechet, J. Convergent dendrons and dendrimers: From synthesis to applications. *Chem. Rev.* **2001**, *101*, 3819–3868.
32. Singh, R.; Lillard, J.W. Nanoparticle-based targeted drug delivery. *Exp. Mol. Pathol.* **2009**, *86*, 215–223.

33. Bogart, L.K.; Pourroy, G.; Murphy, C.J.; Puntes, V.; Pellegrino, T.; Rosenblum, D.; Peer, D.; Lévy, R. Nanoparticles for imaging, sensing, and therapeutic intervention. *ACS Nano* **2014**, *8*, 3107–3122.
34. Zhu, X.; Radovic-Moreno, A.F.; Wu, J.; Langer, R.; Shi, J. Nanomedicine in the management of microbial infection—Overview and perspectives. *Nano Today* **2014**, *9*, 478–498.
35. Huh, A.J.; Kwon, Y.J. "Nanoantibiotics": A new paradigm for treating infectious diseases using nanomaterials in the antibiotics resistant era. *J. Control. Release* **2011**, *156*, 128–145.
36. Kalhapure, R.S.; Suleman, N.; Mocktar, C.; Seedat, N.; Govender, T. Nanoengineered drug delivery systems for enhancing antibiotic therapy. *J. Pharm. Sci.* **2015**, *104*, 872–905.
37. Pelgrift, R.Y.; Friedman, A.J. Nanotechnology as a therapeutic tool to combat microbial resistance. *Adv. Drug Deliv. Rev.* **2013**, *65*, 1803–1815.
38. Lu, H.D.; Spiegel, A.C.; Hurley, A.; Perez, L.J.; Maisel, K.; Ensign, L.M.; Hanes, J.; Bassler, B.L.; Semmelhack, M.F.; Prud'homme, R.K. Modulating Vibrio cholerae quorum-sensing-controlled communication using autoinducer-loaded nanoparticles. *Nano Lett.* **2015**, *15*, 2235–2241.
39. D'Addio, S.M.; Baldassano, S.; Shi, L.; Cheung, L.; Adamson, D.H.; Bruzek, M.; Anthony, J.E.; Laskin, D.L.; Sinko, P.J.; Prud'homme, R.K. Optimization of cell receptor-specific targeting through multivalent surface decoration of polymeric nanocarriers. *J. Control. Release* **2013**, *168*, 41–49.
40. O'Toole, G.A. Microtiter dish biofilm formation assay. *J. Vis. Exp.* **2011**, *47*, 2437.
41. Han, J.; Zhu, Z.; Qian, H.; Wohl, A.R.; Beaman, C.J.; Hoye, T.R.; Macosko, C.W. A Simple Confined Impingement Jets Mixer for Flash Nanoprecipitation. *J. Pharm. Sci.* **2012**, *101*, 4018–4023.
42. Müsken, M.; Di Fiore, S.; Römling, U.; Häussler, S. A 96-well-plate–based optical method for the quantitative and qualitative evaluation of Pseudomonas aeruginosa biofilm formation and its application to susceptibility testing. *Nat. Protoc.* **2010**, *5*, 1460–1469.
43. Heydorn, A.; Nielsen, A.T.; Hentzer, M.; Sternberg, C.; Givskov, M.; Ersbøll, B.K.; Molin, S. Quantification of biofilm structures by the novel computer program COMSTAT. *Microbiology* **2000**, *146*, 2395–2407.
44. Vorregaard, M. Comstat2—A Modern 3D Image Analysis Environment for Biofilms, in Informatics and Mathematical Modelling. Master's Thesis, Technical University of Denmark, Kongens Lyngby, Denmark, 31 January 2008. Available online: www.comstat.dk (accessed on 4/23/2019).